A table of n-component handlebody links of genus n+1 up to six crossings

(Article begins on next page)

03 May 2024

Terms of use:

A TABLE OF n-COMPONENT HANDLEBODY LINKS OF GENUS $n+1$ UP TO SIX CROSSINGS

GIOVANNI BELLETTINI, GIOVANNI PAOLINI, MAURIZIO PAOLINI,
AND YI-SHENG WANG

ABSTRACT. A handlebody link is a union of handlebodies of positive genus embedded in 3-space, which generalizes the notion of links in classical knot theory. In this paper, we consider handlebody links with a genus two handlebody and $n-1$ solid tori, $n > 1$. Our main result is the classification of such handlebody links with six crossings or less, up to ambient isotopy.

1. INTRODUCTION

Early works on knot tabulation, motivated by Kelvin's vortex theory, can be traced back as early as the 19th. To date, all prime knots up to 16 crossings are classified [5], [10]. Knot tabulation has been further generalized to other contexts in recent years. [24] and [26] tabulate prime theta curves and handcuff graphs up to seven crossings, and based on this, [14] subsequently enumerates all irreducible handlebody knots of genus two up to six crossings. The primary goal of knot tabulation is to classify embedded objects by their complexity. At the same time it provides abundant examples, allowing us to better understand knot properties, such as topology and symmetry of knot complements.

The aim of this paper is to extend the classification of handlebody knots of genus two in [14] (see also [20], [15]) to handlebody *links* with $n > 1$ components having total genus $n+1$ (Table 1); we call such a handlebody link an $(n,1)$-handlebody link; it consists of exactly one genus two handlebody and $n-1$ solid tori. Our classification theorem is based on classifications of minimal diagrams and of not necessarily connected spatial graphs with small crossing number (compare with [24], [25]).

While the chirality of some handlebody knots in [14] is hard to detect [27], [20], [12], [15], and remains unknown for some of them [13], the chirality of all handlebody links in Table 1 can be determined. The investigation also reveals that complements of handlebody links can behave quite differently; there are irreducible $(n,1)$-handlebody links, $n > 2$, with ∂-reducible complements, a phenomenon not occurring with handlebody knots of genus two (see [34] and Remark 3.3). The following theorems summarize the main results of the paper.

Theorem 1.1. *Table 1 enumerates all non-split[1], irreducible[2] $(n,1)$-handlebody links, up to ambient isotopy and mirror image, by their minimal diagrams, up to six crossings.*

---

[1]A handlebody link HL is split if there is a 2-sphere $\mathfrak{S} \subset \mathbb{S}^3$ with $\mathfrak{S} \cap \text{HL} = \emptyset$ separating HL into two parts.

[2]A handlebody link HL is reducible if there is a 2-sphere $\mathfrak{S} \subset \mathbb{S}^3$ with $\mathfrak{S} \cap \text{HL}$ an incompressible disk in HL.

4_1 and 5_1 in Table 1 are the only non-split, irreducible $(n, 1)$-handlebody links with four and five crossings, respectively. Among the 15 handlebody links with six crossings, some of them have $n > 2$ components. We remark that 6_5 in Table 1 represents the famous *figure eight puzzle* devised by Stewart Coffin [3]. Thus, its unsplittability implies the impossibility of solving the puzzle (Remark 3.2). Also, $(6_2, 6_4)$ and $(6_{11}, 6_{14})$ are pairs of inequivalent handlebody links with homeomorphic complements.

Our task with respect to Table 1 is two-fold: We need to show firstly that there is no extraneous entry, that is, all entries in the table

U.1 represent non-split handlebody links,
U.2 represent irreducible handlebody links,
U.3 are mutually inequivalent, up to mirror image,
U.4 attain minimal crossing numbers.

and secondly that the table is *complete*, namely no missing handlebody links with crossing number $c \leq 6$.

In Section 3 we prove U.1-U.3, making use of invariants such as the linking number [23], irreducibility criteria [2], and the Kitano-Suzuki invariant [17] (Theorems 3.2, 3.7, and 3.1, respectively). We prove the completeness of Table 1 by exhausting all—except for those obviously non-minimal—diagrams of non-split, irreducible $(n, 1)$-handlebody links up to six crossings (Section 4).

Observe that the underlying plane graph of a diagram of a non-split, irreducible $(n, 1)$-handlebody link necessarily has edge connectivity 2 or 3. For the sake of simplicity, we say a diagram has connectivity e if its underlying plane graph has edge connectivity e. Diagrams with connectivity 3 up to six crossings are generated by a computer code (Appendix A), whereas handlebody links represented by diagrams with connectivity 2 are recovered by employing the knot sum—the *order*-2 *vertex connected sum*—of spatial graphs [24]. In more detail, a minimal diagram D with connectivity 2 can be decomposed by decomposing circles[3] into simpler tangle diagrams, each of which induces a spatial graph that admits a minimal diagram with connectivity 3 or 4, as illustrated in Fig. 1.1. This decomposition allows us to recover the handlebody link represented by D by performing the *knot sum* between prime links and a *spatial graph* that admits a minimal diagram with connectivity 3.
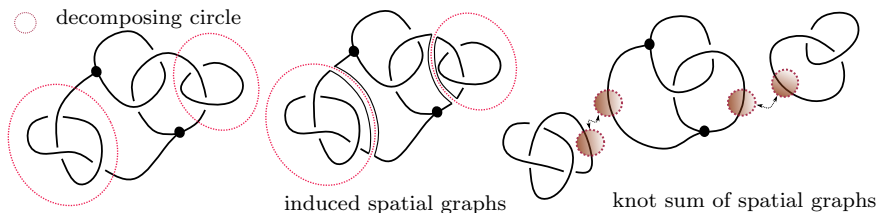
FIGURE 1.1. Decomposing a minimal diagram with connectivity 2.

Once a list containing all possible minimal diagrams of non-split, irreducible handlebody links is produced, we examine each entry on the list manually (Appendix A), and show that it either is non-minimal or represents a handlebody link ambient isotopic to one in Table 1 with the same crossing number, up to mirror image. This proves the completeness, and also implies U.4 by induction on crossing number.

---

[3]a circle that intersects D at two different arcs.

Theorem 1.2. 5_1, 6_3, 6_6, 6_7, 6_8, 6_{10} *are the only chiral handlebody links in Table 1.*

The proof of Theorem 1.2 occupies Section 5.2, and the main tool is Theorem 5.2, where we prove a uniqueness result for decomposition of non-split, irreducible handlebody links with no genus $g > 2$ component, in terms of order-2 connected sum (Definition 5.1). A unique decomposition theorem in a more general form for handlebody knots of arbitrary genus is given in [18, Appendix B] (see also [15]).

Theorem 1.3. *Table 5 enumerates all non-split, reducible $(n, 1)$-handlebody links up to six crossings, up to ambient isotopy and mirror image.*

Theorem 1.3 follows from the irreducibility of handlebody links in Table 1 and a uniqueness factorization theorem (Theorem 6.1) for non-split, reducible $(n, 1)$-handlebody links in terms of order-1 connected sum (Definition 6.1).

The structure of the paper is the following. Basic properties of handlebody links are reviewed in Section 2. Uniqueness, unsplittability, and irreducibility of handlebody links in Table 1 are examined in Section 3. The completeness of Table 1 is discussed in Section 4. Section 5 introduces the notion of decomposable handlebody links, and uses it to examine the chirality of handlebody links in Table 1. A classification of non-split, reducible handlebody links up to six crossings is given in Section 6. Section 7 concludes the paper with a discussion of questions arising from the work. In the appendix we include an analysis on the output of the code available at `http://dmf.unicatt.it/paolini/handlebodylinks/`.

Throughout the paper we work in the PL category; for the illustrative purposes, the drawings often appear smooth. In the case of 3-dimensional submanifolds in $\mathbb{S}^3$, the PL category is equivalent to the smooth category due to [4, Theorem 5], [9, Theorems 7.1, 7.4], [28, Theorem 8.8, 9.6, 10.9].

2. Preliminaries

2.1. **Handlebody links and spatial graphs.**

Definition 2.1 (**Embeddings in $\mathbb{S}^3$**)**.** A handlebody link HL (resp. a spatial graph G) is an embedding of finitely many handlebodies of positive genus (resp. a finite graph[4]) in the oriented 3-sphere $\mathbb{S}^3$.

The *genus* of a handlebody link is the sum of the genera of its components; a spatial graph is *trivalent* if the underlying graph is trivalent (each vertex has degree 3). By a slight abuse of notation, we also use HL (resp. G) to denote the image of the embedding in $\mathbb{S}^3$. The mirror image of HL (resp. G) is denoted by rHL (resp. rG).

Definition 2.2 (**Equivalence**)**.** Two handlebody links HL, HL' (resp. spatial graphs G, G') are equivalent if they are ambient isotopic; they are equivalent up to mirror image if HL (resp. G) is equivalent to HL' or $r\mathrm{HL}'$ (resp. G' or $r\mathrm{G}'$).

A regular neighborhood of a spatial graph defines a handlebody link, up to equivalence [31, 3.24], and a spine of a handlebody link HL is a spatial graph $\mathrm{G} \subset \mathrm{HL}$ such that HL is a regular neighborhood of G [11]. Here we are mainly concerned with trivalent spines.

Lemma 2.1. *Every handlebody link admits a (trivalent) spine.*

---

[4]A finite graph is a graph with finitely many vertices and edges; to exclude trivial objects, we require that no component has positive Euler characteristic. A circle is regarded as a graph without vertices as in [11].

Table 1. Non-split, irreducible handlebody links up to six cross-ings.
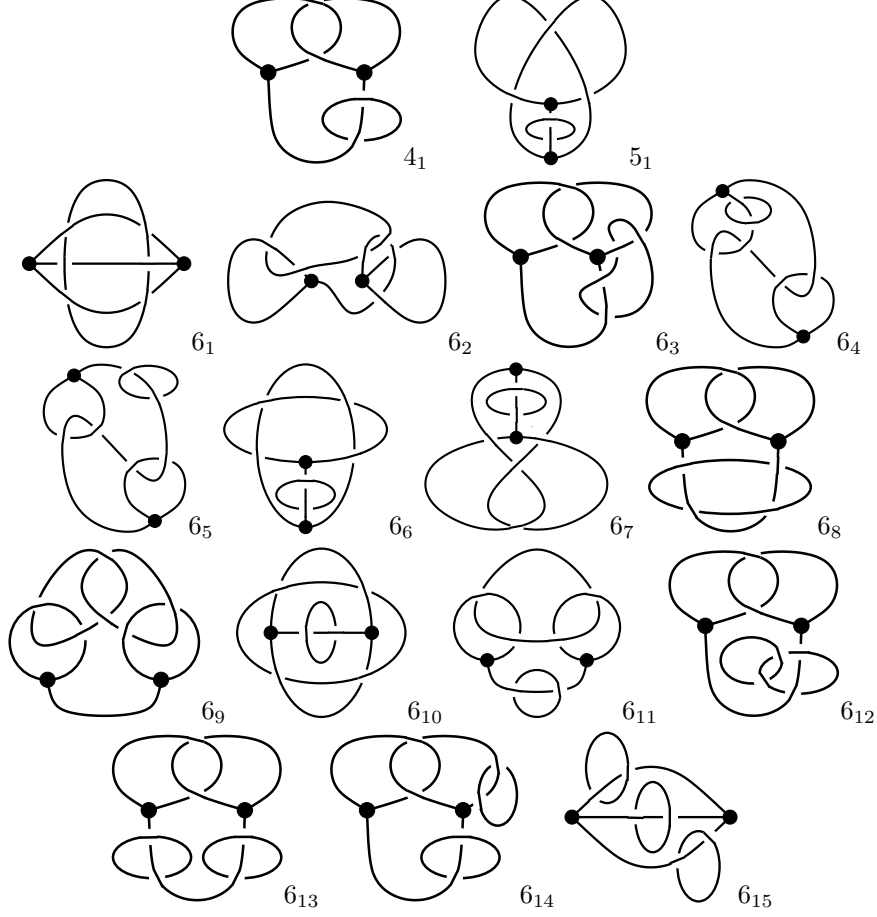
Proof. It suffices to prove the connected case. Suppose HK is a handlebody knot of genus g, and $\mathbf{D} = \{D_1, \cdots, D_{3g-3}\}$ is a set of disjoint incompressible disks in HK such that the complement of the tubular neighborhoods $N(D_i)$ of D_i in HK consists of 3-balls $B_i, i = 1, \cdots, 2(g-1)$, each of which intersects with $\coprod_{i=1}^{3g-3} \partial \overline{N(D_i)}$ at three disks. Note that such a disk system always exists.

Let disks D_{i1}, D_{i2}, D_{i3} be components of $B_i \cap \left(\bigcup_{k=1}^{3g-3} \overline{N(D_k)} \right)$, and choose points v_{i1}, v_{i2}, v_{i3} in the interior of D_{i1}, D_{i2}, D_{i3} and a point v_i in the interior of B_i. Then, joining v_i to v_{ij} by a path for each j gives us a trivalent vertex. Repeat the construction for every i, and then glue the v_{ij} together so that the vertices v_{ij} and $v_{i'j'}$ are identified if they are in the same $\overline{N(D_k)}$, for some k. This way, we obtain a connected trivalent spine of HK with $2(g-1)$ trivalent vertices. $\square$

In general, a trivalent spine of a n-component handlebody link of genus g has $2(g-n) = 2t$ trivalent vertices, and we call such a handlebody link a (n, t)-handlebody link. This paper is primarily concerned with the case $t = 1$.

2.2. **Diagrams.** Let $\mathbb{S}^k = \mathbb{R}^k \cup \infty$. Without loss of generality, it may be assumed handlebody links or spatial graphs are away from ∞.

Definition 2.3 (**Regular projection**). A regular projection of a spatial graph G is a projection $\pi : \mathbb{S}^3 \setminus \infty \to \mathbb{S}^2 \setminus \infty$ such that the set $\pi^{-1}(x) \cap$ G is finite with

its cardinality $\#(\pi^{-1}(x) \cap G) \leq 2$ for any $x \in \mathbb{S}^2 \setminus \infty$, and no 0-simplex of the polygonal subset G of $\mathbb{S}^3$ is in the preimage of a double point, a double point being a point $x \in \mathbb{S}^2 \setminus \infty$ with $\#(\pi^{-1}(x) \cap G) = 2$.

As with the case of knots, up to ambient isotopy, every spatial graph admits a regular projection: the idea is to choose a vector v neither parallel to a 1-simplex in the polygonal subset $G \subset \mathbb{R}^3 = \mathbb{S}^3 \setminus \infty$ nor in a plane containing a 0-simplex and a 1-simplex or two 1-simplices; then isotopy G slightly to remove those points x with $\#\pi_v^{-1}(x) \cap G > 2$, where π_v is the projection onto the plane normal to v.

Definition 2.4 (**Diagram of a spatial graph**)**.** A diagram of a spatial graph G is the image of a regular projection of G with relative height information added to each double point.

The convention is to make breaks in the line corresponding to the strand passing underneath; thus each double point becomes a *crossing* of the diagram.

Definition 2.5 (**Diagram of a handlebody link**)**.** A diagram of a handlebody link HL is a diagram of a spine of HL.

A diagram of G (resp. HL) is trivalent if it is obtained from a regular projection of a trivalent spatial graph (resp. spine).

Definition 2.6 (**Crossing number**)**.** The crossing number $c(D)$ of a diagram D of a handlebody link HL (resp. of a spatial graph G) is the number of crossings in D. The crossing number $c(\text{HL})$ of HL (resp. $c(\text{G})$ of G) is the minimum of the set

$$\{c(D) \mid D \text{ a diagram of HL (resp. G)}\}.$$

Definition 2.7 (**Minimal diagram**)**.** A minimal diagram D of a handlebody link HL (resp. of a spatial graph G) is a diagram of HL (resp. G) with $c(D) = c(\text{HL})$ (resp. $c(D) = c(\text{G})$).

Every multi-valent vertex in a minimal diagram D can be replaced with some trivalent vertices by the inverse of the contraction move [11, Fig. 1] without changing the crossing number, so for a handlebody link (resp. a spatial graph) there always exists a trivalent minimal diagram. From now on, we use the term "a diagram" to refer to a *trivalent* diagram of either a spatial graph or a handlebody link.

Now, regarding each crossing in a diagram as a quadrivalent vertex, we obtain a plane graph, a finite graph embedded in the 2-sphere. If we work backward, and start with a plane graph having only trivalent and quadrivalent vertices, we can produce diagrams by replacing quadrivalent vertices with under- or over-crossings. If the plane graph has $2t$ trivalent vertices and c quadrivalent vertices, then from it we can recover 2^{c-1} diagrams, up to mirror image. In particular, a c-crossing (n, t)-handlebody link can be recovered from one of these plane graphs. Therefore, if one can enumerate all plane graphs with $2t$ trivalent vertices and up to c quadrivalent vertices, then one can recover all (n, t)-handlebody links up to c crossings.

2.3. Moves.

Definition 2.8 (**Moves**)**.** Local changes in a diagram depicted in Fig. 2.1 and Fig. 2.2 are called generalized Reidemeister moves, and the local change in Fig. 2.3 is called an IH-move.

Note that spines of equivalent handlebody links might be inequivalent as spatial graphs; indeed, the following holds.

Theorem 2.2 ([16, Theorem 2.1], [36])**.** *Two trivalent spatial graphs are equivalent if and only if their diagrams are related by a finite sequence of generalized Reidemeister moves.*

Theorem 2.3 ([11, Corollary 2])**.** *Two handlebody links are equivalent if and only if their trivalent diagrams are related by a finite sequence of generalized Reidemeister moves and IH-moves.*
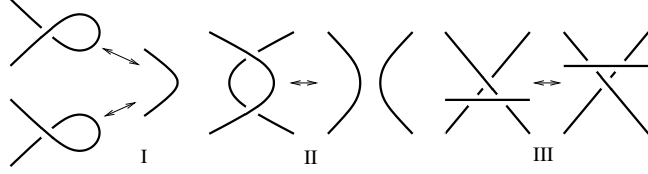

FIGURE 2.1. Classical Reidemeister moves of type I, II, III.
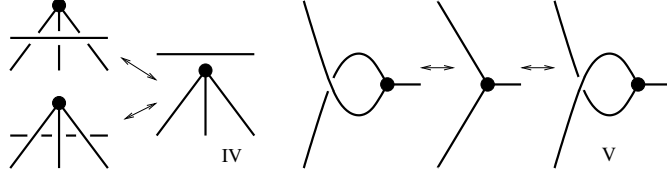
FIGURE 2.2. Reidemeister moves IV and V involve a trivalent vertex.
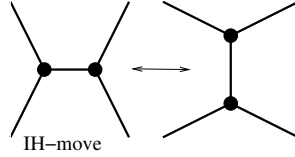
FIGURE 2.3. The IH-move.

When analyzing the data from the code (Section 4 and Appendix A), we adopt the convention: a diagram is called *IH-minimal* if the number of crossings cannot be reduced by generalized Reidemeister moves and IH moves, that is, "minimal" as a diagram of a *handlebody link*, and a diagram is called *R-minimal* if the number of crossings cannot be reduced by generalized Reidemeister moves, that is, "minimal" as a diagram of a *spatial graph*.

2.4. **Non-split, irreducible handlebody links.**

Definition 2.9 (**Edge connectivity of a graph**)**.** The edge-connectivity of a graph is the minimum number of edges whose deletion disconnects the graph.

Definition 2.10 (**Connectivity of a diagram**)**.** A diagram has connectivity e if its underlying plane graph has edge-connectivity e.

Definition 2.11 (**Split handlebody link**)**.** A handlebody link HL is split if there exists a 2-sphere $\mathfrak{S} \subset \mathbb{S}^3$ such that $\mathfrak{S} \cap \mathrm{HL} = \emptyset$ and both components of the complement $\overline{\mathbb{S}^3 \setminus \mathfrak{S}}$ have non-trivial intersection with HL.

Definition 2.12 (**Reducible handlebody link**)**.** A handlebody link HL is reducible if its complement admits a 2-sphere $\mathfrak{S}$ such that $\mathfrak{S} \cap \mathrm{HL}$ is an incompressible disk in HL; otherwise it is irreducible.

Note that $\mathfrak{S}$ in Definition 2.12 factorizes HL into two handlebody links, each of which is called a *factor* of the factorization of HL.

A diagram with connectivity 0 (resp. connectivity 1) represents a split (resp. reducible) handlebody link, so only diagrams with connectivity greater than 1 are of interest to us; on the other hand, the connectivity of a diagram of a (n, t)-handlebody link with $t > 0$ cannot exceed 3.

Now, we recall the order-2 vertex connected sum between spatial graphs [24] for producing handlebody links represented by minimal diagrams with connectivity 2. A trivial ball-arc pair of a spatial graph G is a 3-ball B with $G \cap B$ a trivial tangle in B; it is oriented if an orientation of $G \cap B$ is given.

Definition 2.13 (**Knot sum**). Given two spatial graphs G_1, G_2 with oriented trivial ball-arc pairs B_1, B_2 of G_1, G_2, respectively, their order-2 vertex connected sum $(G_1, B_1) \# (G_2, B_2)$ is a spatial graph obtained by removing the interiors of B_1, B_2 and gluing the resulting manifolds $\overline{\mathbb{S}^3 \setminus B_1}$ and $\overline{\mathbb{S}^3 \setminus B_2}$ by an orientation-reserving homeomorphism

$$h : \left(\partial(\overline{\mathbb{S}^3 \setminus B_1}), \partial(G_1 \cap B_1) \right) \to \left(\partial(\overline{\mathbb{S}^3 \setminus B_2}), \partial(G_2 \cap B_2) \right).$$

The notation $G_1 \# G_2$ denotes the set of order-2 vertex connected sums of G_1, G_2 with all possible trivial ball-arc pairs.

Since an order-2 vertex connected sum depends only on the edges of G_1, G_2 intersecting with B_1, B_2 and their orientations, $G_1 \# G_2$ is a finite set.

3. Uniqueness, non-splittability, and irreducibility

Recall that, given a finite group G, the Kitano-Suzuki invariant $ks_G(HL)$ of a handlebody link HL is the number of conjugate classes of homomorphisms from $\pi_1(\overline{\mathbb{S}^3 \setminus HL})$ to G [17]. Table 2 lists the invariants $ks_{A_4}(HL)$ and $ks_{A_5}(HL)$ of each handlebody link HL in Table 1, as well as an upper bound of the rank of $\pi_1(\overline{\mathbb{S}^3 \setminus HL})$ computed by Appcontour [29], where A_k is the alternating group on k letters.

The entry "split" refers to the split handlebody link HL given by a trivial handlebody knot and an unknotted solid torus; the entry "fake 6_5" is the split handlebody link consisting of the handlebody knot HK 4_1, Ishii-Kishimoto-Suzuki-Moriuchi's 4_1 in [14], and an unknotted solid torus; the entry "fake 6_{11}" is 6_{11} in Table 1 with one of the bottom crossings reversed, thus making the lower solid torus component split off.

Theorem 3.1 (**Uniqueness**). *Entries in Table 1 are all inequivalent.*

Proof. All entries in Table 1 except for the pairs $(6_2, 6_4)$ and $(6_{11}, 6_{14})$ are distinguished by comparing their ks_{A_4}- and ks_{A_5}-invariants (shown in Table 2). On the other hand, 6_2 and 6_4 cannot be equivalent because the removal of the "unknot" component produces inequivalent handlebody knots: one being trivial, the other being HK 4_1. Similarly, one can distinguish 6_{11} and 6_{14} by removing the solid torus component having a non-trivial linking number with the genus two handlebody component [23] in each of them, and observing that, for 6_{14}, the resulting handlebody link is 4_1, whereas for 6_{11}, we get the trivial split handlebody link. $\square$

Remark 3.1. The pairs $(6_2, 6_4)$ and $(6_{11}, 6_{14})$ in fact have homeomorphic complements, and hence the fundamental group cannot discriminate. Fig. 3.1 and 3.2 illustrate how to obtain the complements of 6_2 and 6_{11} from 6_4 and 6_{14}, respectively, via twisting (indicated by arrows).

Remark 3.2. 6_5 viewed as a diagram of a spatial graph is the notorious figure eight puzzle devised by Stewart Coffin [3]. The goal of the puzzle is to free the circle

TABLE 2. Kitano-Suzuki invariant for entries in Table 1.

handlebody link	components	ks_{A_4}	ks_{A_5}	rank
split	trivial + unknot	178	3675	3
4_1	trivial + unknot	114	600	3
5_1	trivial + unknot	98	660	≤ 4
6_1	trivial + unknot	90	600	3
6_2	trivial + unknot	106	689	3
6_3	trivial + unknot	90	469	3
6_4	HK4$_1$ + unknot	106	689	3
6_5	HK4$_1$ + unknot	210		≤ 4
fake 6_5	HK4$_1$ + unknot	274		
6_6	trivial + unknot	130	1380	3
6_7	trivial + unknot	98	597	≤ 4
6_8	trivial + unknot	114	1401	3
6_9	trivial + 2 unknots	310	1841	4
6_{10}	trivial + 2 unknots	326		4
6_{11}	trivial + 2 unknots	486	5876	4
fake 6_{11}	trivial + 2 unknots	694		
6_{12}	trivial + 2 unknots	502	5883	4
6_{13}	trivial + 2 unknots	822		4
6_{14}	trivial + 2 unknots	486	5876	4
6_{15}	trivial + 3 unknots	1242		5

component from the knotted handcuff graph, i.e. to obtain the fake 6_5 as a spatial graph. The impossibility of solving the puzzle then follows from computing $ks_{A_4}(\bullet)$ of 6_5 and fake 6_5 (Table 2). See [1], [22] for other proofs of this.
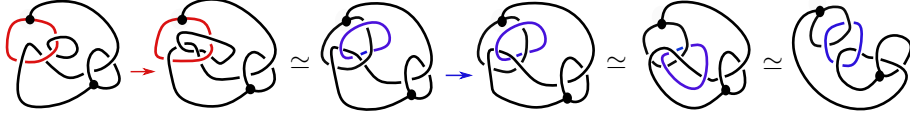
FIGURE 3.1. 6_2 and 6_4 have homeomorphic complements.

FIGURE 3.2. 6_{11} and 6_{14} have homeomorphic complements.

Theorem 3.2 (Unsplittability). *Entries in Table 1 are all unsplittable.*

Proof. In most cases $(5_1, 6_1, 6_2, 6_3, 6_4, 6_7, 6_9, 6_{10})$ unsplittability follows by computing the linking number [23] between pairs of components of a handlebody link. There are a few cases where the linking number vanishes, and we deal with these cases by computing the ks_{A_4}- and ks_{A_5}-invariants of the corresponding split handlebody links (Table 2).

If 6_5 were split, then 6_5 would be equivalent to the fake 6_5 but this is not possible by Table 2. In the case of 4_1, 6_6, 6_8, if any of them were split, than it would be

equivalent to "split" in Table 2, but that is not the case. A similar argument can be applied to 6_{11} and 6_{14}: if one of them were split, it would be equivalent to the fake 6_{11}, in contradiction to Table 2. Lastly, we observe that 6_{12} and 6_{13} are non-split, for otherwise 4_1 would be split. $\qquad\square$

Below we recall the irreducibility test developed in [2]. An r-generator link is a link whose knot group, the fundamental group of its complement, is of rank r.

Lemma 3.3. *If the trivial knot is a factor of some factorization of a reducible $(n, 1)$-handlebody link* HL*, then*

$$12 \mid ks_{\mathsf{A}_4}(\text{HL}) + 6 \cdot 3^n + 2 \cdot 4^n \quad \textbf{\textit{and}} \quad 60 \mid ks_{\mathsf{A}_5}(\text{HL}) + 14 \cdot 4^n + 19 \cdot 3^n + 22 \cdot 5^n. \quad (3.1)$$

Lemma 3.4. *If a 2-generator knot is factor of some factorization of a reducible $(n, 1)$-handlebody link* HL*, then*

$$12 + 24p \mid ks_{\mathsf{A}_4}(\text{HL}) + (6 + 16p) \cdot 3^n + (2 + 6p) \cdot 4^n, \textbf{ where } p = 0 \textbf{ or } 1. \quad (3.2)$$

Lemma 3.5. *If a 2-component, 2-generator link is a factor of some factorization of a reducible $(n, 1)$-handlebody link* HL*, then*

$$48 + 24p \mid ks_{\mathsf{A}_4}(\text{HL}) + (26 + 16p) \cdot 3^{n-1} + (8 + 6p) \cdot 4^{n-1}, \textbf{ where } p = 0, 1, 2, 3 \textbf{ or } 4. \quad (3.3)$$

From the above lemmas, one derives the following irreducibility test (see [2] for more details), making use of the Grushko theorem [8].

Corollary 3.6 (**Irreducibility test**)**.** *A 3-generator $(2, 1)$-handlebody link is irreducible if it fails to satisfy* (3.1)*; a 4-generator $(2, 1)$-handlebody link is irreducible if it fails to satisfy* (3.2)*; a 4-generator $(3, 1)$-handlebody link or a 5-generator $(4, 1)$-handlebody link is irreducible if it fails to satisfy* (3.1) *and* (3.3)*.*

Theorem 3.7 (**Irreducibility**)**.** *Entries in Table1 are irreducible.*

Proof. Corollary 3.6, together with Table 2, shows that all but 6_9, 6_{12} are irreducible. The irreducibility of 6_{12} and 6_9 follows from computing the linking number between each pair of components in each of them. Specifically, if 6_{12} (resp. 6_9) is reducible, then either the trivial knot or a 2-generator 2-component link is a factor of some factorization of 6_{12} (resp. 6_9). For 6_{12}, the former case is not possible by (3.1); the latter impossible too, for otherwise the two solid torus components would have a trivial linking number. The same argument implies that 6_9 cannot have a 2-generator 2-component link as a factor, and the trivial knot cannot be its factor either, since the homomorphism of integral homology

$$H_1(V_1) \oplus H_1(V_2) \to H_1(\overline{\mathbb{S}^3 \setminus W})$$

is onto, where V_1, V_2 are the solid torus components, and W the genus two component. $\qquad\square$

Remark 3.3. The complement of 6_9 is in fact ∂-reducible; one can see this by performing the twist operation, indicated by the arrow in Fig. 3.3a, where it shows that its complement is homeomorphic to the complement of the order-1 connected sum (Definition 6.1) between two Hopf links (Fig. 3.3a, right). The same argument implies that Fig. 3.3b is an irreducible $(m + 3, 1)$-handlebody link with ∂-reducible complement, $m \geq 0$.
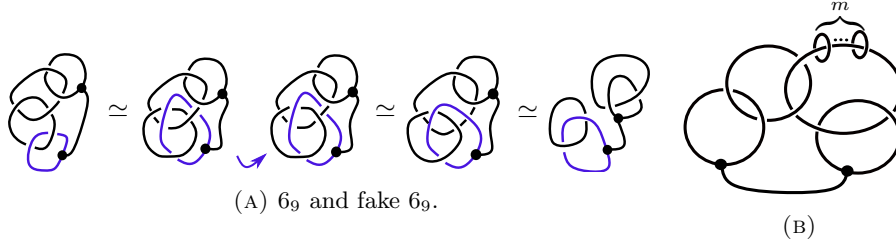
(A) 6_9 and fake 6_9.

(B)

FIGURE 3.3. Irreducible handlebody links with a ∂-reducible complement.

4. COMPLETENESS

This section discusses completeness of Table 1. Recall first that a minimal diagram of a non-split, irreducible handlebody link has either connectivity 2 or 3. IH-minimal diagrams with connectivity 3 are obtained from a software code, and handlebody links represented by IH-minimal diagrams with connectivity 2 are recovered by knot sum of spatial graphs.

4.1. **Minimal diagrams with connectivity 3.** We consider plane graphs with two trivalent vertices and up to six quadrivalent vertices satisfying the properties:

(1) each of them has edge-connectivity 3 as an abstract graph,
(2) their double arcs can only connect two quadrivalent vertices as abstract graphs, and
(3) their double arcs only form a "bigon" (a polygon with two sides; the case 'i' in Fig. 4.1) as plane graphs.

The reason of considering only double arcs connecting two quadrivalent vertices with a bigon configuration is because all the other cases lead to either non-R-minimal diagrams or diagrams with connectivity less than 3 (see Fig. 4.1, where "d, e, f, g, h" illustrate those double arcs connecting at least one trivalent vertex and "j, k, l" those connecting two quadrivalent vertices with a non-bigon configuration.)
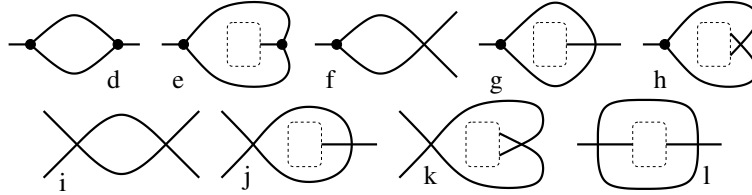
FIGURE 4.1. Possible configurations for loops and double arcs.

We enumerate such plane graphs by the software code, and then recover diagrams from these plane graphs by adding an over- or under-crossing to each quadrivalent vertex. Note that the number (n in Table 3) of components of the associated spatial graphs is independent of how over/under-crossings are chosen. To provide a glimpse of how the code works, we record in Table 3 the number of such plane graphs with c quadrivalent vertices for each n. To recover $(n, 1)$-handlebody links with $n > 1$ represented by IH-minimal diagrams with connectivity 3, we need to consider the cases with $n > 1$ in Table 3. On the other hand, to produce $(n, 1)$-handlebody links represented by IH-minimal diagrams with connectivity 2, spatial graphs admitting an R-minimal diagram with connectivity 3 up to 4 crossings are required; thus all cases with $c \leq 4$ have to be examined.

TABLE 3. Plane graphs given by the code.

c	$n = 1$	$n = 2$	$n = 3$	total
2	1			1
3	2	1		3
4	8	2		10
5	29	8		37
6	144	34	3	181

IH-minimal diagrams. We examine IH-minimality of diagrams produced by plane graphs with $n \geq 2$, and discard those obviously not IH-minimal. This excludes all diagrams produced by the code up to 5 crossings (Table 7), but for diagrams with 6 crossings, some diagrams are potentially IH-minimal: they represent handlebody links 6_1, 6_2, 6_3 or 6_9 in Table 1.
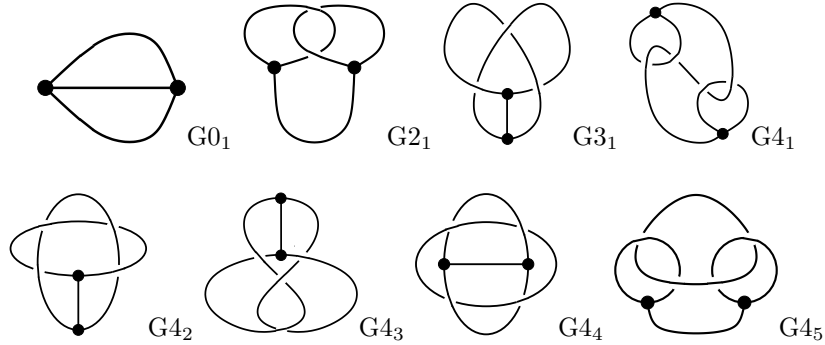
Lemma 4.1. *An IH-minimal diagram with connectivity 3 has crossing number $c \geq 6$, and if $c = 6$, it represents a handlebody link equivalent to 6_1, 6_2, 6_3 or 6_9, up to mirror image.*

Note that we cannot conclude diagrams of $6_1, 6_2, 6_3$ and 6_9 in Table 1 are IH-minimal yet, as they might admit diagrams with connectivity 2 and fewer crossings.

R-minimal diagrams. To produce minimal diagrams with connectivity 2 up to 6 crossings, we need R-minimal diagrams up to 4 crossings. Inspecting R-minimality of diagrams produced by the code (Table 6) gives us the following lemma.

Lemma 4.2. *An R-minimal diagram with connectivity 3 and crossing number less than 5 represents one of the spatial graphs in Table 4, up to mirror image.*

TABLE 4. Spatial graphs up to four crossings.

4.2. **Minimal diagrams with connectivity 2.** Recall a diagram D with 2-connectivity can be decomposed into finitely many simpler tangle diagrams such that each associated diagram of spatial graphs has connectivity 3 or 4 (Fig. 1.1). Furthermore, if D is R-minimal, each induced spatial graph diagram is also R-minimal. In particular, an IH-minimal diagram with connectivity 2 can be recovered by performing the order-2 vertex connected sum between spatial graphs admitting a minimal diagram with connectivity $k > 2$. Since we are interested in $(n, 1)$-handlebody links, only one summand is a spatial graph with two trivalent vertices, and the rest are links admitting a minimal diagram with connectivity 4. Note that the simplest minimal diagram with connectivity 4 represents the Hopf link, and since we only consider minimal diagrams up to 6 crossings, there are at most three link

summands. Thus, IH-minimal diagrams with connectivity 2 can be recovered by considering the seven possible configurations below:

(1) $G \# L_1$,

(2) $(G \# L_1) \# L_2$,

(3) $G \# (L_1 \# L_2)$,

(4) $((G \# L_1) \# L_2) \# L_3$,

(5) $(G \# L_1) \# (L_2 \# L_3)$,

(6) $(G \# (L_1 \# L_2)) \# L_3$,

(7) $G \# ((L_1 \# L_2) \# L_3)$,

where G is a spatial graph admitting a minimal diagram with connectivity 3, and L_i is a link admitting a minimal diagram with connectivity 4. In general it is not known if a minimal diagram with connectivity 4 always represents a prime link; it is the case, however, when crossing number is less than 5. In fact, there are only four minimal diagrams with connectivity 4 up to 4 crossings, and they represent the Hopf link, the trefoil knot, the figure eight, and Solomon's knot (L4a1), respectively.

Cases 4 **through** 7 are easily dealt with since G must have no crossings, and hence it is the trivial theta curve $G0_1$, and thus each L_i is necessarily the Hopf link, so the knot sums actually consist in 'inserting a ring' somewhere to the result of the previous knot sums. To produce irreducible handlebody links there is only one possibility, that is, adding one Hopf link to each of the three arcs of the trivial theta curve, and this gives us entry 6_{15} in Table 1.

Cases 2 **and** 3 force G to have 2 crossings at most. It cannot have zero crossing ($G0_1$), for otherwise, it produces only reducible handlebody links. On the other hand, there is no R-minimal diagram with 1 crossing, and one R-minimal diagram with 2 crossings, this is, $G2_1$ in Table 4 (Moriuchi's 2_1 in [25]).

Now, to add two Hopf links to $G2_1$, namely to place two rings successively, we observe that one of them must be placed around the connecting arc of the handcuff graph by irreducibility. The second ring can be placed in three inequivalent ways, which yield entries 6_{12}, 6_{13} and 6_{14} of Table 1.

Case 1 is more complicated, and we divided it into subcases based on the crossing number $c := c(G)$. The case $c = 0$ is immediately excluded by irreducibility, so three possibilities remain: $c \in \{2, 3, 4\}$.

Subcase $c(G) = 2$. G is necessarily $G2_1$ in Table 4, and L cannot be a knot. Since the crossing number of L cannot exceed 4, L is either L2a1 (Hopf link) or L4a1 (Solomon's knot). In either case, L is to be added to the connecting arc of the handcuff graph to produce irreducible handlebody links, yielding entries 4_1 and 6_8 in Table 1.

Subcase $c(G) = 3$. G is necessarily $G3_1$ (Moriuchi's theta curve 3_1 in [24]), so L cannot be a knot, and hence is the Hopf link. There is only one place to add L by irreducibility, and this leads to entry 5_1 in Table 1.

Subcase $c(G) = 4$. In this case, L has to be the Hopf link; and there are five possible spatial graphs for G, namely $G4_1$, $G4_2$, $G4_3$, $G4_4$, and $G4_5$:

- For $G4_1$ in Table 4 (Moriuchi's non-prime handcuff graph $2_1 \#_3 2_1$ [26]), there are two inequivalent ways to add L which produce entries 6_4 and 6_5.
- For $G4_2$ and $G4_3$ in Table 4 (Moriuchi's prime handcuff graph 4_1 [25] and prime theta-curve 4_1 [24], respectively), there is only one way to add the Hopf link in each case because of irreducibility, and this gives 6_6, 6_7 in Table 1, respectively.
- For $G4_4$ and $G4_5$ in Table 4, again by irreducibility, there is only one way to add the Hopf link in each case, which result in 6_{10} and 6_{11} in Table 1, respectively.

We summarize the above discussion in the following:

Lemma 4.3. *A non-split, irreducible handlebody link admitting an IH-minimal diagram with connectivity 2 and crossing number $c \leq 6$ is equivalent, up to mirror image, to one of the following handlebody links:*

$$4_1, 5_2, 6_4, 6_5, 6_6, 6_7, 6_8, 6_{10}, 6_{11}, 6_{12}, 6_{13}, 6_{14}. \tag{4.1}$$

By Lemma 4.1, if any of (4.1) admits an IH-minimal diagram with connectivity 3, it is equivalent to one of $6_1, 6_2, 6_3,\ 6_9$, while by Lemma 4.1 if $6_1, 6_2, 6_3$ or 6_9 admits an IH-minimal diagram with connectivity 2 and less than 6 crossings, it is equivalent to 4_1 or 5_1, but neither situation can happen by Theorem 3.1.

Corollary 4.4. *Diagrams in Table 1 are all IH-minimal.*

5. CHIRALITY

5.1. **Decomposable links.** Here we consider order-2 connected sum of handlebody-link-disk pairs; compare with Definition 6.1. A handlebod-link-disk pair is a handlebody link HL with an oriented incompressible disk $D \subset$ HL. A trivial knot with a meridian disk is regarded as a trivial handlebody-link-disk pair.

Definition 5.1 (**Order-2 connected sum**)**.** Given two handlebody-link-disk pairs (HL_1, D_1), (HL_2, D_2) the order-2 connected sum $(\mathrm{HL}_1, D_1)\#(\mathrm{HL}_2, D_2)$ is obtained as follows: choose for each i a 3-ball neighborhood B_i of D_i in $\mathbb{S}^3$ with $\mathring{B}_i \cap \mathrm{HL}_i$ a tubular neighborhood $N(D_i)$ of D_i in HL_i. Next, identify $\overline{N(D_i)}$ with $D_i \times [0,1]$ via the orientation of D_i. Then $(\mathrm{HL}_1, D_1)\#(\mathrm{HL}_2, D_2)$ is given by removing $\mathring{B}_i$ and gluing the resulting manifolds via an orientation-reversing homeomorphism:

$$h : \partial(\overline{\mathbb{S}^3 \setminus B_1}) \to \partial(\overline{\mathbb{S}^3 \setminus B_2}) \quad \textbf{with } h(D_1 \times \{j\}) = D_2 \times \{k\}, \ k \equiv j+1 \ \textbf{mod } 2.$$

A handlebody link is *decomposable* if it is equivalent to an order-2 connected sum of some non-trivial handlebody-link-disk pairs.
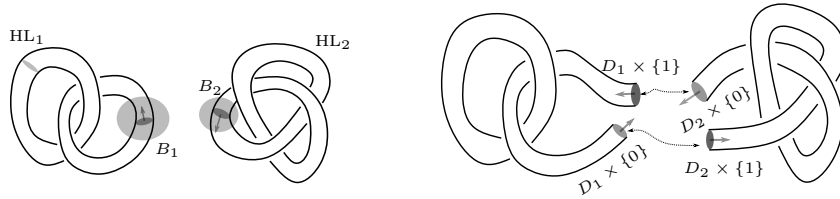
FIGURE 5.1. Knot sum of handlebody-link-disk pairs

Lemma 5.1. *Given a non-split, irreducible handlebody link* HL, HL *is decomposable if and only if* $\overline{\mathbb{S}^3 \setminus \mathrm{HL}}$ *admits an incompressible, ∂-incompressible annulus A with ∂A inessential in* HL.

Proof. This follows from the definition of (∂-) incompressibility. $\qquad\square$

The "∂-incompressible" above can be replaced with "non-boundary parallel" in view of the irreducibility of HL.

Definition 5.2. A properly embedded annulus A in $\overline{\mathbb{S}^3 \setminus \mathrm{HL}}$ is a decomposing annulus of HL (resp. of (HL, D)) if A is incompressible and ∂-incompressible (with $A \cap \partial D = \emptyset$), and ∂A is inessential in HL.

Theorem 5.2. *Given a non-split, irreducible handlebody link* HL *with no component of* HL *having genus* $g \geq 2$, *suppose* A, A' *are decomposing annuli inducing*

$$\text{HL} \simeq (\text{HL}_1, D_1) \# (\text{HL}_2, D_2), \ \text{HL} \simeq (\text{HL}'_1, D'_1) \# (\text{HL}'_2, D'_2), \ \textbf{\textit{respectively}}, \quad (5.1)$$

and $(\text{HL}_i, D_i), i = 1, 2$, *admit no decomposing annulus. Then* A *and* A' *are isotopic, in the sense that there exists an ambient isotopy* $f_t : \mathbb{S}^3 \to \mathbb{S}^3$ *fixing* HL *with* $f_1(A) = A'$.

Proof. Note first that if A, A' are disjoint, then the assumption implies that they must be parallel and hence isotopic. Suppose $A \cap A' \neq \emptyset$. Then we isotopy A such that the number of components of $A \cap A'$ is minimized.

Claim: any circle or arc in $A \cap A'$ is essential in both A and A'. Observe first that a circle component C or an arc component l of $A \cap A'$ is either essential in both A and A' or inessential in both A and A' by the incompressibility and ∂-incompressibility of A and A'.

Suppose C is inessential in both A and A', and is innermost in A'. Then C bounds disks D, D' in A, A', respectively. Since HL is non-split, $D \cup D'$ bounds a 3-ball B in $\overline{\mathbb{S}^3 \setminus \text{HL}}$. Isotopy D across B to D' induces a new annulus A isotopic to the original one with $A \cap A'$ having less components, contradicting the minimality.

Suppose l is inessential in both A and A' and an innermost arc in A'. Then l cuts off a disk D' from A' and a disk D from A. Let $\hat{D} := D \cup D'$. If $\partial\hat{D}$ is inessential, then we can remove the intersection l by isotopying A across the ball bounded by $\hat{D}$ and the disk bounded by $\partial\hat{D}$ in ∂ HL, contradicting the minimality.

If $\partial\hat{D}$ is essential, then isotopying $\hat{D}$, we can disjoin $\hat{D}$ from A. Now, it may be assumed that D_1 is in a genus one component of HL_1, and hence D_2 is in a component of HL_2 with genus $g \leq 2$. Since $\partial\hat{D}$ is essential, $\hat{D}$ has to be in a genus two component of HL_2 containing D_2. Because $\partial\hat{D} \cap D_2 = \emptyset$, if $\partial\hat{D}$ is essential on the boundary of the embedded solid torus $(\text{HL}_2 \setminus N(D_2)) \subset \mathbb{S}^3$, $\partial\hat{D}$ would be its longitude, where $N(D_2)$ is a tubular neighborhood of D_2, disjoint from $\hat{D}$, in HL_2. Particularly, HL_2 and therefore HL would be reducible, a contradiction. On the other hand, if $\partial\hat{D}$ bounds a disk on $\partial(\text{HL}_2 \setminus N(D_2))$ that contains some components of $\partial\overline{N(D_2)}$, then $\partial\hat{D}$ is inessential in HL_2, and hence in HL, again contradicting the irreducibility of HL.

The claim is proved, and $A \cap A'$ contains either essential circles or essential arcs.

No essential circles. Suppose C is an essential circle, and a closest circle to $\partial A'$. Let R' be the annulus cut off by C from A' with $A \cap R' = C$ and R an annulus cut off by C from A. We isotopy the incompressible annulus $\hat{R} := R \cup R'$ away from A. Since components of $\partial\hat{R}$ are inessential in HL, by the assumption, $\hat{R}$ is either parallel to A or boundary-parallel. In the former case, replacing A with R leads to a contradiction since $R \cap A'$ has less components than $A \cap A'$. In the latter case, isotopying R through the solid torus V bounded by $\hat{R}$ and the part of ∂HL parallel to $\hat{R}$ gives a new A isotopic to the original one but with less components in $A \cap A'$, contradicting the minimality.

No essential arcs. Suppose l_1 is an essential arc. Then choose the essential arc l_2 next to l_1 in A' such that the disk D' cut off by l_1, l_2 from A' has $D' \cap A = l_1 \cup l_2$ and is on the side of A containing components of HL_1. Let D be a disk cut off by l_1, l_2 from A. It may be assumed, by pushing D away from A, that $D \cup D'$ is disjoint from A, and hence is on the genus one complement of HL_1 containing D_1. Since $\hat{A} := D \cup D'$ is disjoint from D_1, it is necessarily an annulus, for if it were a Möbious band, we would get a non-orientable surface embedded in $\mathbb{S}^3$. Furthermore, each component of $\partial\hat{A}$ is necessarily inessential in HL_1, so it either bounds a meridian disk or is inessential in ∂ HL_1. Note also it cannot be the case that one component

of $\partial \hat{A}$ is essential in $\partial \mathrm{HL}_1$ and the other inessential by the irreducibility of HL. Suppose both components are inessential in $\partial \mathrm{HL}_1$. Then $\hat{A}$, together with disks on $\partial \mathrm{HL}_1$ bounded by $\partial \hat{A}$, bounds a 3-ball, with which we can isotopy A to remove the intersection l_1, l_2, contradicting the minimality. Suppose both components bound meridian disks in HL_1. Then $\tilde{A} = D^c \cup D'$ has $\partial \tilde{A}$ inessential in $\partial \mathrm{HL}_1$, where $D^c = \overline{A \setminus D}$. Thus we reduce it to the previous case. $\qquad \square$

5.2. Chirality.

We divide the proof of Theorem 1.2 into two lemmas.

Lemma 5.3. *All handlebody links except for* 5_1, 6_3, 6_6, 6_7, 6_8, 6_{10} *in Table 1 are achiral.*

Proof. An equivalence between 6_2 and $r6_2$ is depicted in Fig. 5.2; the chirality of the other handlebody links are easy to see.

FIGURE 5.2. 6_2 and $r6_2$.

$\qquad \square$

Lemma 5.4. 5_1, 6_3, 6_6, 6_7, 6_8, 6_{10} *in Table 1 are chiral.*

Proof. Recall that, given a handlebody link HL, if HL and rHL are equivalent, then there is an orientation-reversing self-homeomorphism of $\mathbb{S}^3$ sending HL to HL.

Observe that each of $5_1, 6_6, 6_8, 6_{10}$ admits an obvious decomposing annulus satisfying conditions in Theorem 5.2; particularly the annulus in each of them is unique. Their chirality then follows readily from the fact that torus links are chiral.

To see chirality of 6_3, we observe that, given a $(2,1)$-handlebody link HL, any self-homeomorphism of $\mathbb{S}^3$ preserving HL sends the meridian m and the preferred longitude l of the circle component to $m^{\pm 1}$ and $l^{\pm 1}$, respectively. In particular, any isomorphism on knot groups induced by such a homeomorphism sends the conjugacy class of $m \cdot l$ in $\pi_1(\overline{\mathbb{S}^3 \setminus \mathrm{HL}})$ to the conjugacy class of $m \cdot l$, $m^{-1} \cdot l$, $m \cdot l^{-1}$ or $m^{-1} \cdot l^{-1}$, depending on whether the homeomorphism is orientation-preserving.

Let N be the number of conjugacy classes of homomorphisms from $\pi_1(\overline{\mathbb{S}^3 \setminus \mathrm{HL}})$ to a finite group G that sends $m \cdot l$ (and hence $m^{-1} \cdot l^{-1}$) to 1, and rN the number of conjugacy classes of homomorphisms from $\pi_1(\overline{\mathbb{S}^3 \setminus \mathrm{HL}})$ to G that sends $m \cdot l^{-1}$ (and hence $m^{-1} \cdot l$) to 1. Now, if HL and its mirror image rHL are equivalent, then $N = rN$. This is however not the case with 6_3; when $\mathsf{G} = A_5$, we have $(N, rN) = (77, 111)$ as computed by [29].
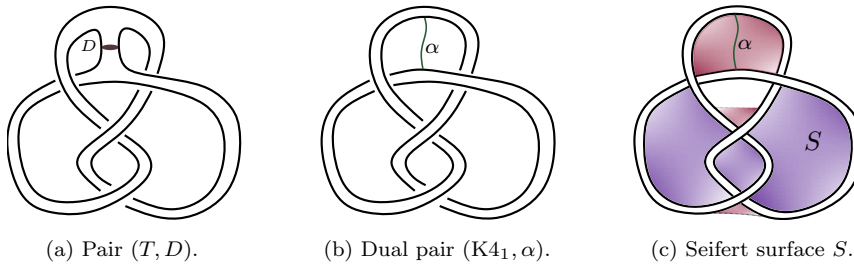

(a) Pair (T, D).   (b) Dual pair $(K4_1, \alpha)$.   (c) Seifert surface S.

FIGURE 5.3. ●

(A) Induced Hopf link.
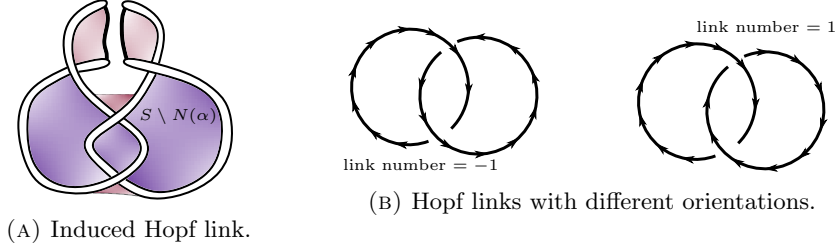
(B) Hopf links with different orientations.

FIGURE 5.4. ●

In the case of 6_7, by Theorem 5.2 every self-homeomorphism f of $\mathbb{S}^3$ sending 6_7 to itself induces a self-homeomorphism f sending the handlebody-knot-disk pair (T, D) in Fig. 5.3a to itself, or equivalently sending the (fattened) figure eight with an arc $(K4_1, \alpha)$ in Fig. 5.3b to itself, where α is the dual one-simplex to D.

Let S be a minimal Seifert surface of the figure eight (Fig. 5.3c) containing the arc α, and D_+, D_- be two disjoint meridian disks containing $\partial \alpha$, respectively. By the standard covering space argument [30], one can assume $f(\partial S) \cap (D_+ \cup D_-) = \partial \alpha = \partial f(\alpha)$, and hence we can further isotopy f such that $f(N(\alpha)) = N(\alpha)$ for some tubular neighborhood $N(\alpha)$ of α in S.

Both complements $S \setminus N(\alpha)$ and $f(S) \setminus N(\alpha)$ are Seifert surfaces of the induced Hopf link (Fig. 5.4a), and up to ambient isotopy, the Hopf link only admits two minimal Seifert surfaces, among which only one is compatible with $N(\alpha)$. Thus $S \setminus N(\alpha)$ and $f(S) \setminus N(\alpha)$ are ambient isotopic. Now if f is orientation-reversing, it implies the two oriented Hopf links in Fig. 5.4b are ambient isotopic, contradicting their link numbers.

□

6. REDUCIBLE HANDLEBODY LINKS

In this section, we show that Table 5 classifies, up to ambient isotopy and mirror image, all non-split, reducible $(n, 1)$-handlebody links up to six crossings (Theorem 1.3). We begin by considering the order-1 connected sum for handlebody links.

6.1. **Order-1 connected sum.** A handlebody-link-component pair (HL, h) is a handlebody link HL with a selected component h of HL.

Definition 6.1 (Order-1 connected sum). Let (HL_1, h_1) and (HL_2, h_2) be two handlebody-link-component pairs. Then their order-1 connected sum (HL_1, h_1)--(HL_2, h_2) is given by removing the interior of a 3-ball B_1 (resp. B_2) in $\mathbb{S}^3$ with $B_1 \cap \partial HL_1 = B_1 \cap \partial h_1$ (resp. $B_2 \cap \partial HL_2 = B_2 \cap \partial h_2$) a 2-disk, and then gluing the resulting 3-manifolds $\overline{\mathbb{S}^3 \setminus B_1}, \overline{\mathbb{S}^3 \setminus B_2}$ via an orientation-reversing homeomorphism $f : (\partial B_1, (\partial B_1) \cap h_1) \to (\partial B_2, (\partial B_2) \cap h_2)$. We use HL_1--HL_2 to denote the set of order-1 connected sums between HL_1, HL_2 with all possible selected components.
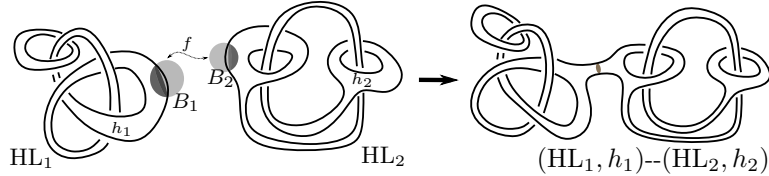
FIGURE 6.1. Order-1 connected sum of (HL_1, h_1)--(HL_2, h_2).

The following generalizes the case of handlebody knots in [34, Theorem 2].

Theorem 6.1 (**Uniqueness**). *Given a non-split, reducible $(n, 1)$-handlebody link HL, if HL $\simeq$ (HL$_1$, h_1)-*-(HL$_2$, h_2), and HL $\simeq$ (HL$'_1$, h'_1)-*-(HL$'_2$, h'_2), then (HL$_i$, h_i) $\simeq$ (HL$'_i$, h'_i), $i = 1, 2$, up to reordering.*

Proof. Note first that, since HL is non-split and reducible, HL$_i$, HL$'_i$, $i = 1, 2$, are non-split, and $\pi_1(\overline{\mathbb{S}^3 \setminus \text{HL}})$ is a non-trivial free product $\mathsf{G}_1 * \mathsf{G}_2$, where G_i is the knot group of HL$_i$, $i = 1, 2$.

Let D and D' be the separating disks in $\overline{\mathbb{S}^3 \setminus \text{HL}}$ given by the factorizations HL $\simeq$ (HL$_1$, h_1)-*-(HL$_2$, h_2) and HL $\simeq$ (HL$'_1$, h'_1)-*-(HL$'_2$, h'_2), respectively. Suppose neither G_1 nor G_2 is isomorphic to $\mathbb{Z}$. Then, up to isotopy, $D' \cap D = \emptyset$ by the innermost circle/arc argument.

Suppose one of G_i, $i = 1, 2$, say G_1, is isomorphic to $\mathbb{Z}$, that is, HL$_1$ is a trivial solid torus in $\mathbb{S}^3$. Then G_2 must be non-cyclic, since $n > 1$. Let D_l be the disk bounded by the longitude of HL$_1$, and isotopy D, D_l such that the number n (resp. n_l) of components of $D' \cap D$ (resp. $D' \cap D_l$) is minimized.

Claim: $n_l = 0$. Note first that the minimality implies that $D' \cap D_l$ contains no circle components. Now, consider a tubular neighborhood $N(D_l)$ of D_l in $\overline{\mathbb{S}^3 \setminus \text{HL}}$ small enough such that $\overline{N(D_l)} \cap D = \emptyset$ and $\overline{N(D_l)} \cap D'$ are some disks, each of which intersects D_l^+ (resp. D_l^-) at exactly one arc on its boundary, where $D_l^{\pm} \subset \partial \overline{N(D_l)}$ are proper disks in $\overline{\mathbb{S}^3 \setminus \text{HL}}$ parallel to D_l. The claim then follows once we have shown that $N(D_l)$ can be isotopied away from D'.

To see this, we construct a labeled tree Υ from the complement of the intersection $D' \cap D_l^{\pm}$ in D', where $D^{\pm} := D_l^+ \cup D_l^-$. Regard each component of $D' \setminus (D' \cap D^{\pm})$ as a node in Υ, and each arc in $D' \cap D_l^{\pm}$ as an edge in Υ connecting the two nodes representing the components of $D' \setminus (D' \cap D^{\pm})$ whose closures intersect at the arc. Since each arc in $D' \cap D^{\pm}$ cuts D' into two, Υ is a tree. The first two figures from the left in Fig. 6.2 illustrate the construction.
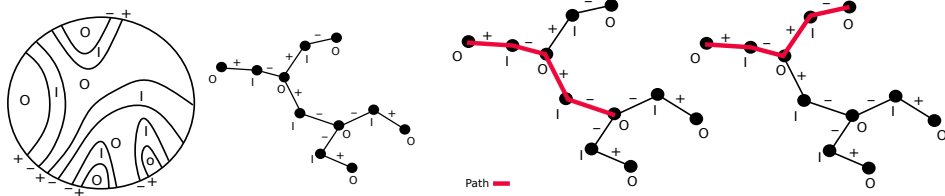

FIGURE 6.2. $h(D_l)$ and Υ.

We label nodes and edges of Υ as follows: A node is labeled with I if the corresponding component of $D' \setminus (D' \cap D^{\pm})$ is inside $N(D_l)$; otherwise the node is labeled with O. An edge of Υ is labeled with $+$ if the corresponding component of $D' \cap D_l^{\pm}$ is in D_l^+; otherwise, it is labeled with $-$.

The labeling on Υ has the following properties: (a) adjacent nodes have different labels; (b) a node with label I is bivalent, and the two adjacent edges are labeled with $+$ and $-$, respectively, whereas a node labeled with O could be multi-valent; (c) a one-valent node corresponds to an innermost arc in D', and always has label O.

Consider a maximal path $\Gamma \subset \Upsilon$ starting from a one-valent node and with the property that adjacent edges of Γ have different labels. Then the other end point of the path must be labeled with O and it is either a one-valent node of Υ or a multi-valent node with all adjacent edges having same label; the two figures from the right in Fig. 6.2 illustrate two possible maximal paths.

Without loss of generality, we may assume that the adjacent edge of the starting one-valent node of Γ is labeled with $+$. Denote the closure of the corresponding component of $D' \setminus \left(D' \cap D^{\pm} \right)$ by D_{Γ}^s. Then ∂D_{Γ}^s bounds a disk T on $\partial(\mathrm{HL} \cup \overline{N(D_l)})$. If $T \cap D_l^- = \emptyset$, then $D_{\Gamma}^s \cap D = \emptyset$ and hence $T \cap D = \emptyset$ by the minimality of n; however, if it were the case, one could reduce n_l by isotopying D_l across the 3-ball bounded by D_{Γ}^s and T. Hence T must contain D_l^-. Since the adjacent edge of the starting node is labeled with $+$, adjacent edges of the end node of Γ in Υ are labeled with $-$. Denote by D_{Γ}^e the closure of the component corresponding to the end node. Then ∂D_{Γ}^e bounds a disk in $\partial(\mathrm{HL} \cup \overline{N(D_l)})$ that is contained in T and has no intersection with D_l^+. Particularly, $D_{\Gamma}^e \cap D = \emptyset$ by the minimality of n, and there is an arc in ∂D_{Γ}^e cutting a disk D'' off $\overline{T \setminus D_l^-}$ with $\mathring{D}'' \cap D' = D'' \cap D = \emptyset$, so one can slide $N(D_l)$ over D'' (Fig. 6.3) to decrease n_l, a contradiction. Consequently,
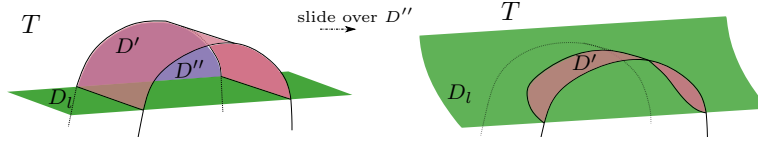

FIGURE 6.3

such a path Γ cannot exist, but this can happen only if Υ is empty. The claim is thus proved. It implies that $\mathrm{HL}_1, \mathrm{HL}_1'$ are trivial solid tori in $\mathbb{S}^3$, and $\mathrm{HL}_2, \mathrm{HL}_2'$ are equivalent to $\overline{N(D_l)} \cup \mathrm{HL}$.   □

TABLE 5. Reducible links with up to six crossings.

crossings	$c(\mathrm{L}_1) + c(\mathrm{L}_2)$	description	$|\mathrm{L}_1\text{-}\mathrm{L}_2|$
2 (1)	$0 + 2$	unknot -- Hopf	1
4 (4)	$0 + 4$	unknot -- L4a1	1
		unknot -- Hopf#Hopf	2
	$2 + 2$	Hopf -- Hopf	1
5 (4)	$0 + 5$	unknot -- Whitehead	1
		unknot -- Trefoil#Hopf	2
	$3 + 2$	trefoil -- Hopf	1
6 (17)	$0 + 6$	unknot -- L6ai, $i = 1, \ldots, 5$	1
		unknot -- L6n1	1
		unknot -- L4a1#Hopf	3
		unknot -- (Hopf#Hopf)#Hopf	4
	$2 + 4$	Hopf -- L4a1	1
		Hopf -- Hopf#Hopf	2
	$4 + 2$	K4a1 -- Hopf	1

6.2. **Non-split, reducible handlebody links.** Table 5 lists all non-split, reducible $(n, 1)$-handlebody links obtained by performing order-1 connected sum on pairs of links $(\mathrm{L}_1, \mathrm{L}_2)$ with crossing numbers (c_1, c_2) and $c_1 + c_2 \leq 6$, the notation $\mathrm{L}{\bullet}a{\bullet}$ or $\mathrm{L}{\bullet}n{\bullet}$ refers to links in the Thistlethwaite link table. Since $n > 1$, one of $\mathrm{L}_1, \mathrm{L}_2$ is a link with more than one component, and by convention we let L_2 be the factor. The number in parentheses indicates the total number of inequivalent reducible handlebody links of the given crossing number. By Theorem 6.1, isotopy types of L_1 and L_2 with selected components determine the isotopy type of the resulting handlebody link in $\mathrm{L}_1\text{-}\mathrm{L}_2$. Thus there are no duplicates in Table 5.

On the other hand, by Lemmas 4.1 and 4.3 and Theorem 3.7, minimal diagrams of non-split, reducible $(n,1)$-handlebody links up to 6 crossings cannot have connectivity $k > 1$. This shows the completeness of Table 5.

7. Perspectives

Our classification of non-split $(n,1)$-handlebody links, and [14], provide examples that shed light on several interesting properties of $(n,1)$-handlebody links. Here we collect some questions arising from the study.

Crossing number. The result in Section 6 implies that every handlebody link in Table 5 admits a minimal diagram with connectivity 1; not *all* their minimal diagrams have connectivity 1 though. Thus we ask the following question.

Question 7.1. *Does every non-split, reducible handlebody link always admit a minimal diagram with connectivity 1?*

An affirmative answer to Question 7.1, together with Theorem 6.1 and [33, Theorem 2], implies the additivity of crossing number, a reminiscence of a one-hundred years old problem in knot theory (see [19], [21] and references therein).

Conjecture 7.2. *If $(\mathrm{HL}_1, h_1)\text{-}\text{-}(\mathrm{HL}_2, h_2)$ is an $(n,1)$-handlebody link, then*

$$c\big((\mathrm{HL}_1, h_1)\text{-}\text{-}(\mathrm{HL}_2, h_2)\big) = c(\mathrm{HL}_1) + c(\mathrm{HL}_2). \tag{7.1}$$

Decomposability. Decomposability is reflected in the connectivity of minimal diagrams in most examples here; in general one may ask the following question.

Question 7.3. *Does every minimal diagram of a non-split, irreducible, decomposable handlebody link have connectivity 2?*

A positive answer to Question 7.3 implies that 6_1, 6_2, 6_3 and 6_9 in Table 1 are indecomposable. As Question 7.3 is expected to be hard, easier methods might be required to determine indecomposability.

Problem 7.4. *Find computable criteria for indecomposability of handlebody links.*

Handlebody link complement. The question of whether irreducibility of a handlebody link implies ∂-irreducibility of its complement has been studied in several situations. In the case of handlebody knot of genus two, this is always true [34, Theorem 1], whereas for handlebody knots of genus $g > 2$, there are counterexamples [32, Example 5.5], [34, Section 5]. Now, Remark 3.3 provides counterexamples in the case of non-split, irreducible $(n,1)$-handlebody links with $n > 2$. We ask whether $n = 2$ is the largest n for such a phenomenon to happen.

Question 7.5. *Is the complement of a non-split, irreducible $(2,1)$-handlebody link always ∂-irreducible?*

Acknowledgements

References

[1] I. Bertuccioni, *A Topological Puzzle*, Amer. Math. Monthly **110** (2003), 937–939.

[2] G. Bellettini, M. Paolini, Y.-S. Wang, *Numerical irreducibility criteria for handlebody links*, arXiv:2002.05974 [math.GT].

[3] J. Botermans, P. Van Delft, *Creative Puzzles of the World*, Abrams, New York, 1975.

[4] M. Brown, *Locally Flat Imbeddings of Topological Manifolds* Ann. Math., Second Series, **75**, (1962), 331–341.

[5] J. H. Conway, *An enumeration of knots and links, and some of their algebraic properties, in Computational Problems in Abstract Algebra*, Proc. Conf. Oxford, (1970), 329–358.

[6] P. R. Cromwell, *Knots and Links*, Cambridge University Press, Cambridge, (2004).

[7] W. Chongchitmate, L. Ng *An atlas of Legendrian knots*, Exp. Math. **22** (2013), no. 1, 26–37.

[8] I. A. Grushko, *On the bases of a free product of groups*, Matematicheskii Sbornik, **8** (1940), 169–182.

[9] M. W. Hirsch, B. Mazur, *Smoothings of Piecewise Linear Manifolds*, (AM-80), Princeton University Press, Princeton, NJ, (1974).

[10] J. Hoste, M. Thistlethwaite, J. Weeks *The first 1,701,936 knots*, Math. Intelligencer **20** (1998), 33–48.

[11] A. Ishii, *Moves and invariants for knotted handlebodies*, Algebr. Geom. Topol. **8** (2008), 1403–1418.

[12] , A. Ishii, M. Iwakiri, *Quandle cocycle invariants for spatial graphs and knotted handlebodies*, Canad. J. Math. **64** (2012), 102–122.

[13] , A. Ishii, M. Iwakiri, Y. Jang, K. Oshiro, *A G-family of quandles and handlebody-knots*, Illinois J. Math. **57** (2013), 817–838.

[14] A. Ishii, K. Kishimoto, H. Moriuchi, M. Suzuki, *A table of genus two handlebody-knots up to six crossings*, J. Knot Theory Ramifications **21** (2012).

[15] A. Ishii, K. Kishimoto, M. Ozawa, *Knotted handle decomposing spheres for handlebody-knots*, J. Math. Soc. Japan **67** (2015), 407–417.

[16] L. H. Kauffman, *Invariants of graphs in three-space*, Trans. Amer. Math. Soc. **311** (1989) (2), 679–710.

[17] T. Kitano, M. Suzuki, *On the number of $SL(2, \mathbb{Z}/p\mathbb{Z})$-representations of knot groups* J. Knot Theory Ramifications **21** (2012).

[18] Y. Koda, M. Ozawa, with an appendix by C. Gordon, *Essential surfaces of non-negative Euler characteristic in genus two handlebody exteriors*, Trans. Amer. Math. Soc. **367** (2015), no. 4, 2875–2904.

[19] M. Lackenby, *The crossing number of composite knots*, J. Topol. **2** (4) (2009), 747–768.

[20] J. H. Lee, S. Lee, *Inequivalent handlebody-knots with homeomorphic complements*, Algebr. Geom. Topol. **12** (2012), 1059—1079.

[21] A. V Malyutin, *On the Question of Genericity of Hyperbolic Knots*, Int. Math. Res. Notices (2018), 1073-7928.

[22] P. Melvin, *A Topological Menagerie*, Amer. Math. Monthly, **113** (2006) 348–351.

[23] A. Mizusawa, *Linking numbers for handlebody-links*, Proc. Japan Acad. **89**, Ser. A (2013), 60–62.

[24] H. Moriuchi, *An enumeration of theta-curves with up to seven crossings* J. Knot Theory Ramifications **18** (2009), 67–197.

[25] H. Moriuchi, *A table of handcuff graphs with up to seven crossings* OCAMI Studies Vol 1. Knot Theory for Scientific objects (2007) 179–300.

[26] H. Moriuchi, *A table of θ-curves and handcuff graphs with up to seven crossings* Adv. Stud. Pure Math. Noncommutativity and Singularities: Proceedings of French–Japanese symposia held at IHES in 2006, J.-P. Bourguignon, M. Kotani, Y. Maeda and N. Tose, eds. (Tokyo: Mathematical Society of Japan, 2009), 281–290.

[27] M. Motto, *Inequivalent genus two handlebodies in S^3 with homeomorphic complements*, Topology Appl. **36**(3) (1990), 283–290

[28] J. Munkres, *Elementary Differential Topology*, (AM-54), Princeton University Press, Princeton, NJ (1966).

[29] M. Paolini, Appcontour. Computer software. Vers. 2.5.3. Apparent contour. (2018) <http://appcontour.sourceforge.net/>.

[30] D. Rolfsen, *Knots and Links*, AMS Chelsea Publishing, vol.364, 2003.

[31] C. P. Rourke, B. J. Sanderson, *Introduction to Piecewise-Linear Topology*, Springer-Verlag, Berlin-New York, (1982).

[32] S. Suzuki, *On surfaces in 3-sphere: prime decompositions*, Hokkaido Math. J. **4** (1975), 179–195.

[33] Y. Tsukui, *On surfaces in 3-space*, Yokohama Math. J. **18** (1970), 93–104

[34] Y. Tsukui, *On a prime surface of genus 2 and homeomorphic splitting of 3-sphere*, The Yokohama Math. J. **23** (1975), 63–75.

[35] H. Whitney, *Congruent graphs and the connectivity of graphs*, Am. J. Math. **54** (1932), 150–168.

[36] D. N. Yetter, *Category theoretic representations of knotted graphs in S^3*, Adv. Math. **77** (1989) 137–155.

APPENDIX A. OUTPUT OF THE CODE

A.1. **Minimal diagrams from the code.** The software code used in the paper exhaustively enumerates 3-edge-connected plane graphs with two trivalent vertices and q quadrivalent vertices, $0 < q \leq 6$, without double arcs that form a non-bigon. Note that the trivial theta curve is the only 3-edge-connected plane graph without quadrivalent vertices. The output of the code is examined and summarized in Table 3, while the detailed list is available on `http://dmf.unicatt.it/paolini/ handlebodylinks/`, where each plane graph is described by its adjacent matrix together with a fixed ordering (clockwise or counterclockwise) of the edges adjacent to every vertex, as determined by the planar embedding.

A.1.1. *Four crossings or less.* In Table 6, we analyze the output of the code up to 4 quadrivalent vertices, where the column "quad. v." lists the number of quadrivalent vertices and "ref. no." the reference number of each plane graph in the output of the code. The column "induced diagrams" describes minimality of diagrams induced by each plane graph. Most induced diagrams are not minimal, and we record those that are and their isotopy types as special graphs or handlebody links, up to mirror image. No IH-minimal diagram with more than one component is found in this case.

TABLE 6. Diagrams with up to 4 crossings.

quad. v.	ref. no.	induced diagrams
1	none	none
2	#1	R-minimal; G2$_1$ in Table 4; not IH-minimal
3	#1,	not R-minimal
	#2,#3	R-minimal; G3$_2$ in Table 4; not IH-minimal
4	#1,#2	IH-minimal; G4$_1$ in Table 4
	#3	R-minimal; G3$_2$ in Table 4; not IH-minimal
	#4, #8	R-minimal; G4$_2$ in Table 4; not IH-minimal
	#5, #6, #7	R-minimal; G4$_3$ in Table 4; not IH-minimal
	#9	R-minimal; G4$_4$ in Table 4; not IH-minimal
	#10	R-minimal; G4$_5$ in Table 4; not IH-minimal

TABLE 7. Diagrams with 5 crossings.

ref. no.	description
#6, #11, #14	not R-minimal
#22, #26, #35	not IH-minimal
#36	not IH-minimal
#37	not R-minimal

A.1.2. *Five and six crossing cases.* In the 5 crossing case, the code finds 8 plane graphs with more than one components, out of a total of 37 planar embeddings.

Table 7 records the analysis for their induced diagrams; none of them gives IH-minimal diagrams. In the 6 crossing case, out of 181 plane graphs, 37 induces diagrams with more than one components. Table 8 records the minimality of their induced diagrams.

TABLE 8. Diagrams with 6 crossings.

ref. no.	description
#5	6_1 in Table 1
#15, #22, #34, #45, #54	not R-minimal
#56	6_1 in Table 1
#60	6_2 in Table 1
#70	6_3 in Table 1
#73	not R-minimal
#83	6_2 in Table 1
#84	6_1 in Table 1
#86, #91, #92, #93	not R-minimal
#104, #105, #114, #117, #123	not IH-minimal
#134, #135, #137, #144	not IH-minimal
#161, #165	6_1 in Table 1
#168, #169, #170,#171	not IH-minimal
#175	6_9 in Table 1
#176	not IH-minimal
#177	not R-minimal
#179, #180	not IH-minimal
#181	6_9 in Table 1

Fig. A.1 exemplifies how the analysis is done. Fig. A.1a shows how the diagrams induced by Plane Graph #5 are equivalent to those by #161 and #165 in the case of 6 crossings, and Fig. A.1b explains non-minimality of diagrams induced by Plane Graphs #168, #169, #170, #171.
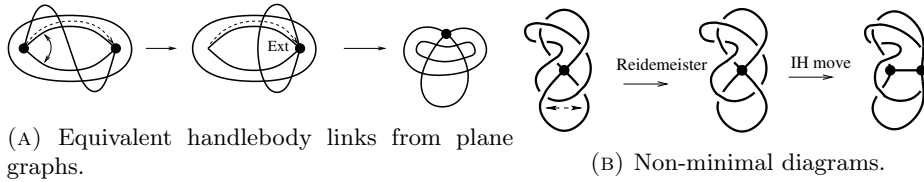

(A) Equivalent handlebody links from plane graphs.

(B) Non-minimal diagrams.

FIGURE A.1. •

A.1.3. *Inequivalent planar embeddings.* As a side remark, Fig. A.2 illustrates two examples of abstract graphs with inequivant planar embeddings: one with five quadrivalent vertices and the other with six. Note that the abstract graphs have vertex connectivity 2, consistent with the Whitney uniqueness theorem [35].

(A) Five-quadrivalent-vertex graph.

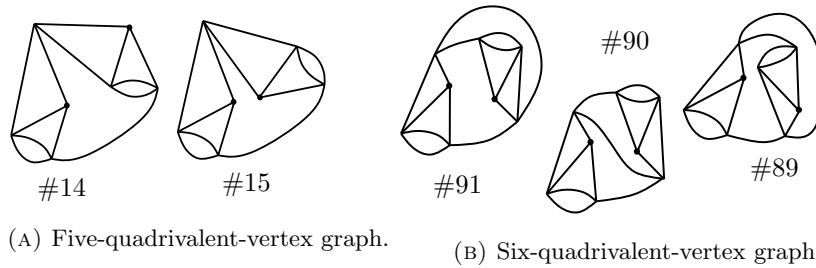(B) Six-quadrivalent-vertex graph.

FIGURE A.2. Inequivalent planar embeddings.

DIPARTIMENTO DI INGEGNERIA DELL'INFORMAZIONE E SCIENZE MATEMATICHE, UNIVERSITÀ DI SIENA, 53100 SIENA, ITALY, AND INTERNATIONAL CENTRE FOR THEORETICAL PHYSICS ICTP, MATHEMATICS SECTION, 34151 TRIESTE, ITALY

Email address: bellettini@diism.unisi.it

CALIFORNIA INSTITUTE OF TECHNOLOGY AND AMAZON WEB SERVICES, PASADENA CA, UNITED STATES (WORK DONE WHILE AT UNIVERSITY OF FRIBOURG, DEPARTMENT OF MATHEMATICS, 1700 FRIBOURG, SWITZERLAND)

Email address: paolini@caltech.edu

DIPARTIMENTO DI MATEMATICA E FISICA, UNIVERSITÀ CATTOLICA DEL SACRO CUORE, 25121 BRESCIA, ITALY

Email address: maurizio.paolini@unicatt.it

INSTITUTE OF MATHEMATICS, ACADEMIA SINICA, TAIPEI 106, TAIWAN

Email address: yisheng@gate.sinica.edu.tw